Quantitative MRI in obesity & reno-cardiovascular function

Dekkers, I.A.

Citation

Dekkers, I. A. (2020, June 18). *Quantitative MRI in obesity & reno-cardiovascular function*. Retrieved from https://hdl.handle.net/1887/119365

Cover Page

Universiteit Leiden

Author: Dekkers, I.A.
Title: Quantitative MRI in obesity & reno-cardiovascular function
Issue Date: 2020-06-18

2

Clinical Application and Technical Considerations of T1 and T2(*) Mapping in Cardiac, Liver, and Renal Imaging

Dekkers IA, Lamb HJ.

ABSTRACT

Pathological tissue alterations due to disease processes such as fibrosis, edema and infiltrative disease can be non-invasively visualized and quantified by magnetic resonance imaging using T1 and T2 relaxation properties. Pixel-wise mapping of T1 and T2 image sequences enable direct quantification of T1, T2(*), and extra-cellular volume (ECV) values of the target organ of interest. Tissue characterization based on T1 and T2(*) mapping is currently making the transition from a research tool to a clinical modality, as clinical usefulness has been established for several diseases such as myocarditis, amyloidosis, Anderson-Fabry and iron deposition. Other potential clinical applications besides the heart include, the quantification of steatosis, cirrhosis, hepatic siderosis and renal fibrosis. Here, we provide an overview of potential clinical applications of T1 and T2(*) mapping for imaging of cardiac, liver and renal disease. Furthermore, we give an overview of important technical considerations necessary for clinical implementation of quantitative parametric imaging, involving data acquisition, data analysis, quality assessment, and interpretation. In order to achieve clinical implementation of these techniques, standardization of T1 and T2(*) mapping methodology and validation of impact on clinical decision making is needed.

2

INTRODUCTION

Pathological alterations in tissue composition often have similar manifestations in different organ systems such as the heart, liver and kidney. To illustrate, fibrotic organs share similarities on both histopathology and imaging, including stiffness due to excessive extracellular matrix deposition, reduced vasculature, and an uneven surface due to fibroblast formation (1, 2). Also edema manifests in different organs as excessive fluid accumulation either within cells (cellular edema) or within the collagen matrix of the interstitial spaces (interstitial edema) (3). Infiltrative diseases (e.g. iron deposition, amyloidosis, and lipid accumulation) can lead to systemic alterations in tissue composition causing dysfunction of different organs, including heart, liver, and kidney. These pathological changes in tissue composition can be non-invasively visualized and quantified using novel multiparametic imaging techniques, whereas conventional MR imaging only enabled qualitative image interpretation and signal intensity based analysis using arbitrary units (4).

Direct quantification of the T1 and T2(*) via parametric imaging (i.e. imaging using quantitative sequences such as T1 and T2(*) mapping with milliseconds as the corresponding unit) addresses several of these limitations via the inherent quantitative results and elimination of user-dependent interpretation. Tissue characterization using late gadolinium enhancement (LGE) in cardiac MR is considered the gold standard non-invasive imaging technique for the assessment of myocardial scar, however several important limitations exist. Since LGE relies on differences in signal intensity between scar tissue and adjacent 'normal' tissue, it is not sensitive for the detection of diffuse fibrosis (5). Additionally, signal intensities in LGE are expressed on an arbitrary scale which challenges comparison over time, and the enhancing tissues are not only influenced by technical parameters during image acquisition but also to the arbitrarily set intensity threshold (6). T2 weighted imaging is commonly used to asses inflammation and edema, however these sequences are affected by various limitations including regional differences introduced by signal variation due to phased-array coil arrays, and difficulties in differentiating edema from sub-endocardial blood in cardiac MR (7). Quantification of T1 and T2 values based on a quantitative pixel-wise maps can reduce the variation in assessment and thus serve as an alternative for LGE and T2 weighted imaging (8). T1 and T2(*) mapping not only identifies and quantifies diseased tissue contents, but also allows for direct comparison over time with reduced analysis time (9). Initial efforts of multiparametric imaging using T1 and T2(*) mapping have mainly focused on cardiac imaging, however these techniques can also be applied in other organs, such as liver, and kidney. This ability of non-invasive tissue characterization could ultimately be used for better understanding of common disease pathways and monitoring of the effectiveness of different therapies. An overview of potential parametric imaging methods for the assessment of different heart, liver and kidney diseases is given in **Table 1**. In this review we provide an overview of the potential

clinical application of T1 and T2(*) mapping for the imaging of cardiac, liver and renal disease. Furthermore, we describe important technical considerations involving data acquisition, data analysis, quality assessment, and interpretation that are necessary for the clinical implementation of quantitative parametric imaging.

Table 1. Overview of potential parametric imaging methods for the assessment of different heart, liver and kidney diseases

Parametric imaging method	Organ of interest		
	Heart	Liver	Kidney
Native T1	edema (acute ischemia, acute inflammation), storage disease (amyloid, iron, lipid deposition)	Fibrosis, steatohepatitis, post-transplantation changes	Fibrosis, post-transplantation changes
ECV, Post-contrast T1	fibrosis (replacement: chronic infarction, primary cardiomyopathy; interstitial; primary cardiomyopathy, volume overload)	Functional liver parenchyma	
T2	edema (acute ischemia, acute inflammation)	edema (preclinical models only)	edema, renal cyst progression (preclinical models only)
T2*	iron deposition	iron deposition	

ECV, extracellular volume.

T1 mapping

T1 mapping is the geographical representation of true T1 of certain tissues within the field of view. In order to reconstruct the T1 map, proton spin-lattice relaxation times (T1) are calculated for every voxel within the field of view using multiple raw images with different degrees of recovery of magnetization along the longitudinal axis following inversion recovery (IR) or saturation recovery (SR) prepulses (10) (**Fig. 1a and 1b**). T1 maps are reconstructed in either colour or gray scale, where the intensity of a certain voxel represents the corresponding T1 value. This voxel-wise T1 mapping has led to numerous studies on the clinical utility of signal quantification for the detection of myocardial disease in cardiac MRI (11). Voxel-wise T1-mapping was first introduced by the inversion recovery based modified look-locker imaging (MOLLI) sequence (12), and has led to the development of shortened MOLLI (shMOLLI) (13), and variations. Saturation recovery based sequences are saturation-recovery single-shot Acquisition (SASHA) (14), and mixed IR-SR combinations such as saturation-pulse prepared heart-rate independent inversion-recovery (SAPPHIRE) (15).

T1 mapping can be used for tissue characterization by: a) native (non-contrast) T1 reflecting tissue disease involving both cellular components as interstitium, or b) extracellular volume fraction (ECV) after the administration of gadolinium based contrast agents. ECV
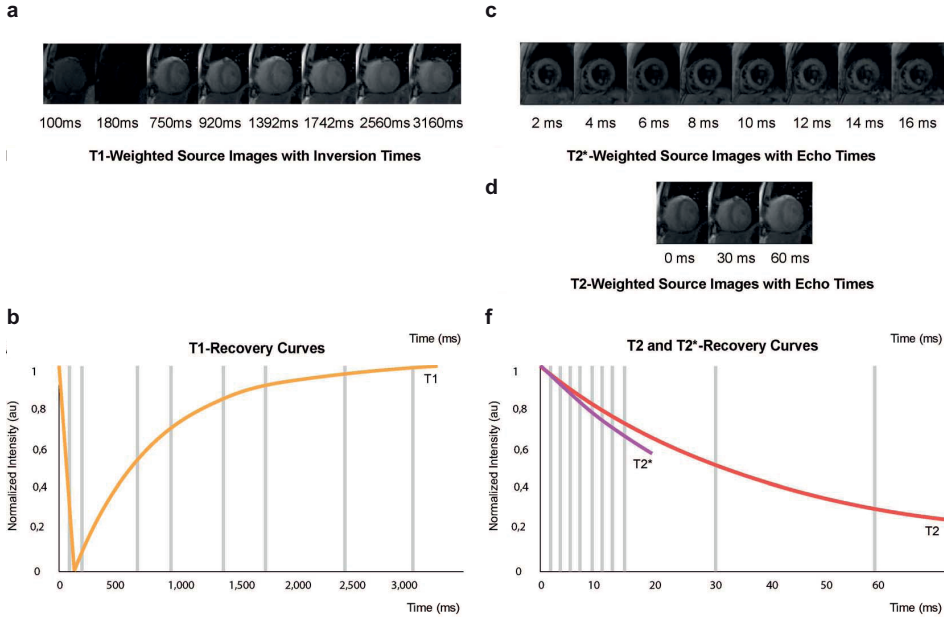
Figure 1. Magnetization Inversion Recovery for T1, T2*, T2 mapping. (**a**) Different images are obtained following an inversion pulse at multiple different inversion times for T1 mapping during the same phase of the cardiac cycle in subsequent heart beats. (**b**) As the inversion time increases the longitudinal magnetization increases due to T1 recovery, yellow curve. (**c**) Different gradient echo images are acquired at different echo times for T2* mapping, and (**d**) different spin-based preparation images are acquired at different echo times for T2 mapping. (**e**) As the TE increases, the myocardial signal intensity decreases due to T2 decay, red curve, and due to static field inhomogeneities for T2* decay, pink curve.

directly quantifies the size of the extracellular space as a percentage reflecting interstitial disease, and is independent of field strength (16). ECV is calculated as follows:

$$ECV\ (\%) = (1 - hematocrit) \times \frac{(\frac{1}{T1\ post,\ tissue} - \frac{1}{T1\ native,\ tissue})}{(\frac{1}{T1\ post,\ blood\ pool} - \frac{1}{T1\ native,\ blood\ pool})}$$

where T1 post is the contrast-enhanced T1 of the tissue of interest or blood pool, T1 tissue native is the non-enhanced T1 of the tissue of interest or blood pool (**Fig. 2**).

T2 and T2* mapping

T2 mapping is the voxel-wise representation of the proton spin-spin relaxation time (T2) of the tissue of interest within the field of view. T2 values for each voxel are acquired via based T2 weighted images at various echo times with a long repetition time in order to minimize the effect of longitudinal relaxation (**Fig. 1c and Fig. 1d**). Acquired T2 values reflect the free water content present in the tissue of interest, which can be used for quantification of edema. The most frequently used sequence for T2 mapping is the balanced steady-state free precession (bSSFP) sequence (8), and other used sequences are

Extracellular volume fraction mapping (ECV)
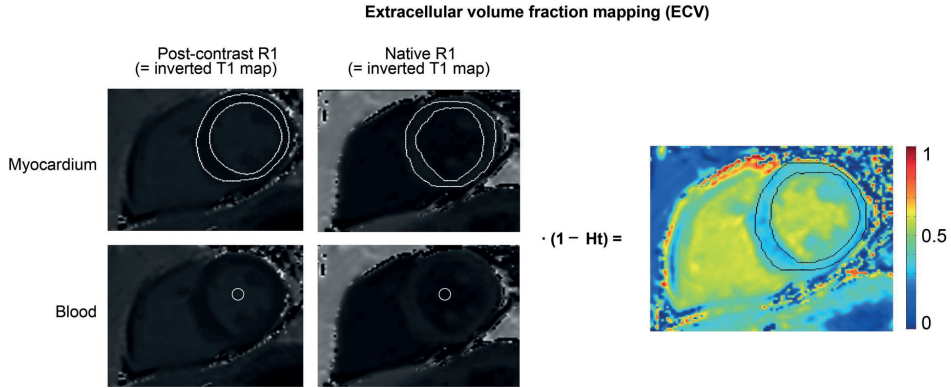
Figure 2. Calculation of ECV. Calculation of ECV using the inverse of the signal in each pixel (1/T1) is used to generate an R_1 map (F). The ΔR_1 map of the blood pool (ΔR_1blood) and myocardium (ΔR_1myocard) is generated by subtracting the corresponding precontrast R_1 map from the postcontrast R_1 map. ΔR_1 map pixel values are multiplied by one minus the hematocrit level, and then divided by the mean ΔR_1blood in order to calculate ECV. The final result is a colour encoded parametric map displaying the pixel-by-pixel ECV values.

gradient-recalled echo (17) and spiral imaging (18). These sequences are combined with several images with different T2 preparation module echo times.

T2 star (denoted as T2*) mapping uses the effective T2 value which decays faster than true T2 due to the dephasing effects of local field inhomogeneities from susceptibility differences present within the voxel (**Fig. 1c and Fig. 1e**). T2* mapping can be used for measurement of iron content in tissues. Used T2* mapping sequences are multi-echo gradient recalled echo (GRE) sequences (19).

CLINICAL APPLICATIONS

Heart

*Diffuse fibrosis and infiltrative cardiac diseases*

One of the major advantages of T1 mapping compared to LGE is the possibility to visualize infiltrative interstitial disease or extensive diffuse fibrosis (**Fig. 3 and Fig. 4**). Fibrosis which is a non-physiological scarring process leading to destruction of organ architecture and organ dysfunction via excessive deposition of extracellular matrix (2). Increased T1 on native, and post-contrast images due to diffuse fibrosis has extensively been described in several diseases, such as hypertrophic cardiomyopathy, aortic stenosis, sarcoidosis, systemic sclerosis, and myocarditis (20) (**Fig. 5**). Also, interstitial myocardial fibrosis after treatment with anthracycline chemotherapy has been associated with significantly increased ECV values compared with oncologic patients that had not yet initiated chemotherapy (21). These findings indicate that T1-mapping techniques may
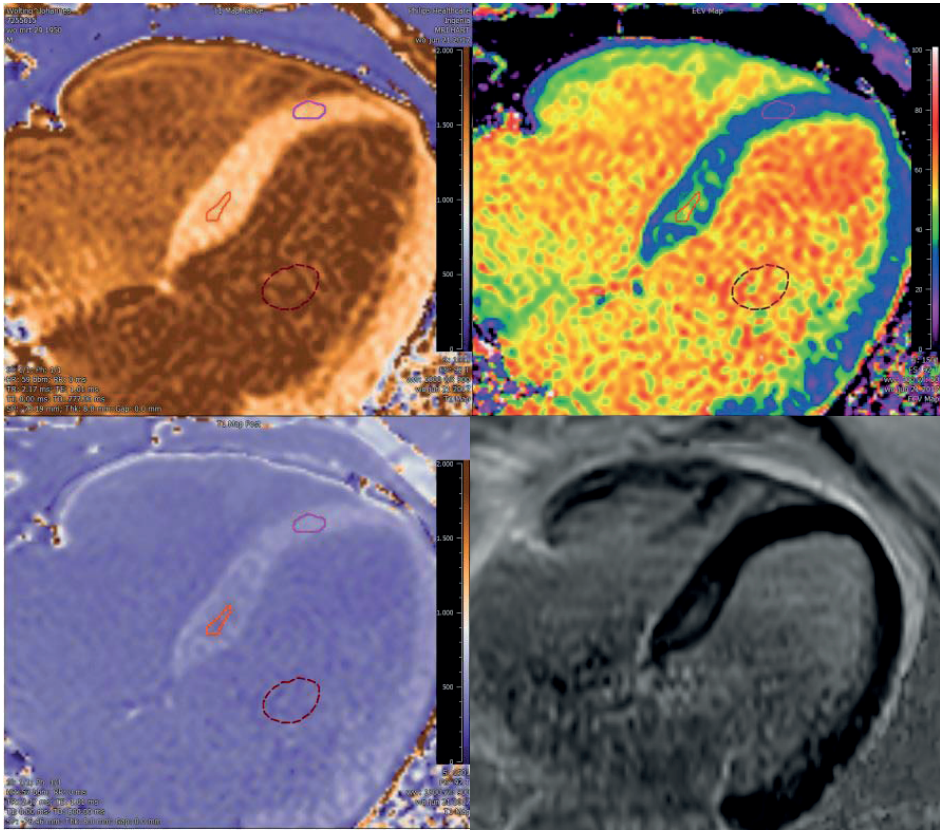
Figure 3. Example of added value ECV of the heart compared to LGE only in a patient with premature ventricular contractions (PVCs). LGE shows some enhancement basal septal, which is confirmed by the ECV map constructed using the pre- and post-contrast T1 maps. The ECV in the region of interest was 45% localized in focal septal hypertrophy, which is the likely origin of the PVC's. Quantitative T1 and ECV maps were automatically reconstructed on a voxel-by-voxel basis after data acquisition using the T1 map processing tool (Medis research, version 3.0, Leiden).

be useful as novel risk stratification biomarkers for cardiotoxicity prior to and during treatment with anthracycline agents. Increased interstitial space does not only result from fibrosis, but may also be due to the presence of infiltrates such as in amyloidosis (22, 23). In amyloidosis, T1 mapping and ECV have made great advance in diagnosing cardiac involvement and have shown to be predictive of mortality (23-25). As such, the necessity of cardiac biopsy for confirming cardiac involvement can be debated as native T1 and ECV can be used reliably for non-invasive diagnosis. Another exemplary disease with diffuse myocardial infiltration that can be well detected via parametric imaging is Anderson-Fabry disease. Anderson-Fabry is characterized by intracellular lysosomal lipid accumulation which results in decreased T1 values on native T1 mapping (26, 27). Other cardiomyopathies in which T1 mapping and ECV have been described to be potentially
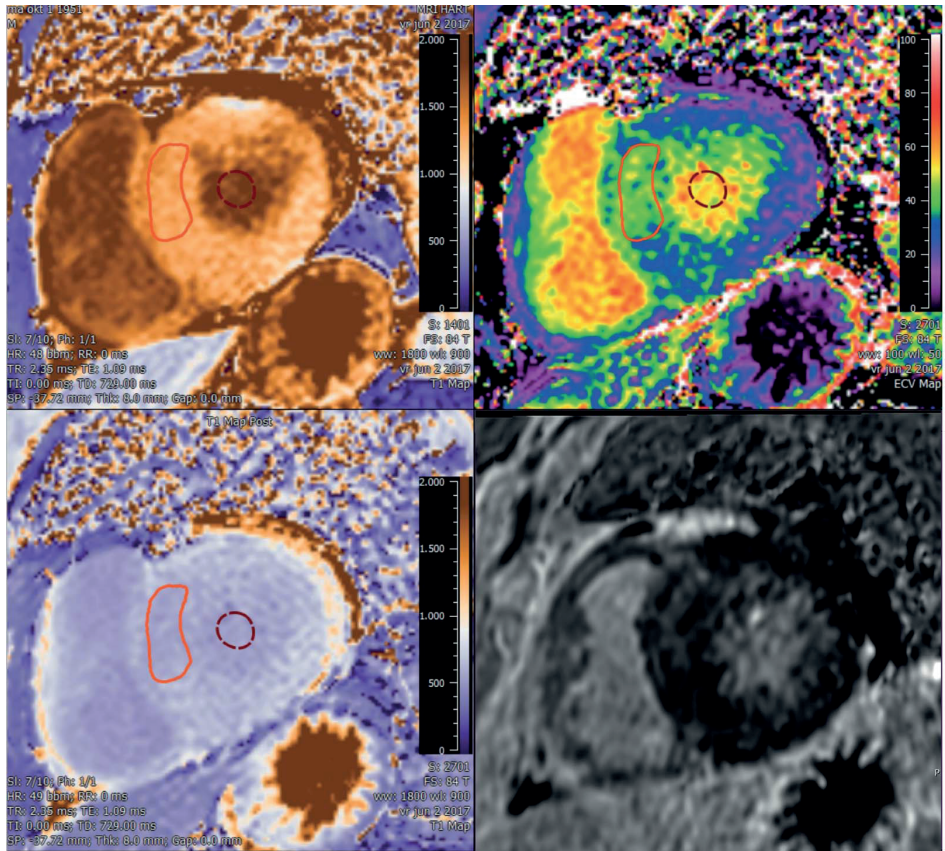
Figure 4. Example of added value of ECV compared to LGE in a patient with familial hypertrophic cardiomyopathy with diffuse fibrosis. Non-dilated left ventricle with septal hypertrophy with diffuse fibrosis (serum haematocrit of 45%, native T1 septum 1315 ms [N<1350 ms], and ECV 42 % [N<35%]). Quantitative T1 and ECV maps were automatically reconstructed on a voxel-by-voxel basis after data acquisition using the T1 map processing tool (Medis research, version 3.0, Leiden).

beneficial for diagnosis are hypertrophic (28) and dilating cardiomyopathy (29), however further research is still needed to validate diagnostic usefulness and prognostication. Another example of an interstitial disease in which T2* mapping can be of great value is cardiac siderosis. Previous research has showed that myocardial T2 values correlate well with tissue iron concentration (30), which has enabled visualization and quantification of iron accumulation in the heart using T2(*) mapping (**Fig. 6a**). Parametric imaging could be besides diagnosis also be used for treatment monitoring, such as plasma cell dyscrasia suppressive agents for light-chain Amyloidosis (31), enzyme replacement therapies for Anderson-Fabry (32), and modern chelation regimes for cardiac cardiac sidersosis (33). Early initiation of chelation therapy based on myocardial T2* has drastically influenced long-term prognosis in patients with thalassemia by decreasing the annual death rate
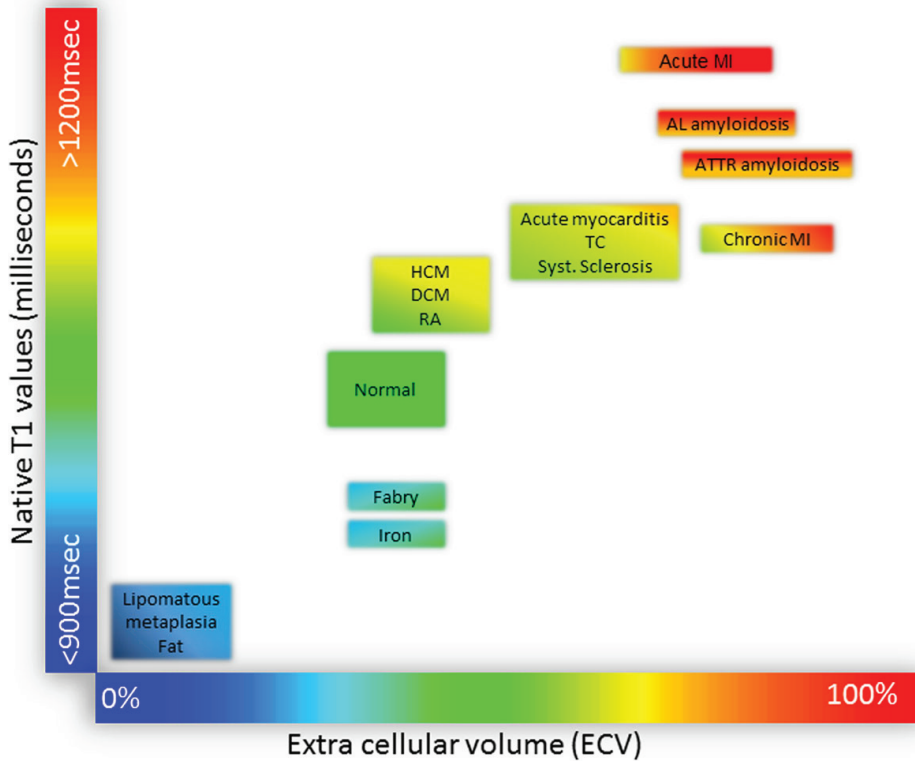
Figure 5. Tissue characterization using native T1 and extracellular volume fraction (ECV). Absolute values for native T1 depend greatly on field strength (1.5 T or 3 T), pulse sequence (MOLLI or ShMOLLI), scanner manufacturer and post-processing. For the purpose of comparability, only studies using 1.5 T scanners were considered in this figure. Reprinted from Haaf P et. al. (95), publisher BioMed Central under the terms of the Creative Commons License.

from cardiac iron overload (33). When available, T1 mapping and ECV could also be used for monitoring the effectiveness of antifibrotic treatments (34).

Cardiac dysfunction

Functional studies have showed that higher ECV values are correlated with reduced left ventricular ejection fraction, and lower myocardial blood flow in dilated cardiomyopathy and lower systolic strain in left ventricular hypertrophy (28, 35). Furthermore, interstitial fibrosis in diastolic dysfunction has also been linked to the development of heart failure with preserved ejection fraction (36). These findings suggest that the expansion of the extracellular matrix may be a key contributor to contractile dysfunction. Combining parametric imaging of the heart with functional cardiac MR imaging could be of great advantage for identifying focal areas of interstitial fibrosis that negatively influence car-
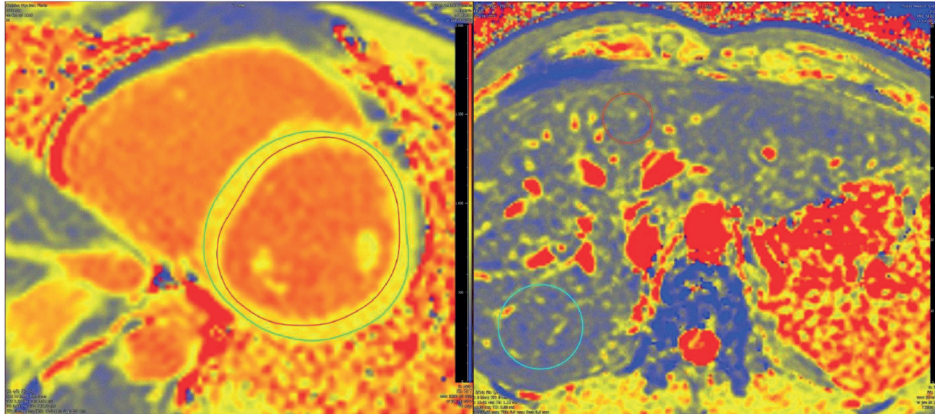
Figure 6. T2* mapping of heart (left) and liver (right) in a childhood cancer survivor at risk of secondary hemosiderosis after multiple blood transfusions and chemotherapy for acute lymphatic leukemia. Parametric imaging of heart and liver using StarQuant (Philips) heart and LiverMultiScan (Perspectum). The myocardial T2* value was 38 ms (normal reference >20 ms), and liver T2* value was 13.3 ms, indicating normal T2* values of the heart and minimal iron deposition in the liver. Quantitative T2 maps were automatically reconstructed on a voxel-by-voxel basis after data acquisition using the T2 map processing tool (Medis research, version 3.0, Leiden).

diac function. There is an growing body of evidence evaluating the prognostic value of T1 mapping and ECV in in patients with cardiac dysfunction (37). Several studies have been performed that evaluated the association between native T1 (38, 39), and ECV (11, 40-42) with incident heart failure and all-cause mortality. These studies have found that both native T1 and ECV are more sensitive for predicting adverse events that left ventricular ejection fraction which is the currently used for prognostication in heart failure (37). However, for T2 mapping thus far no prognostic evidence has been reported for patients with heart failure although the diagnostic role of T2 mapping for acute conditions such as acute myocardial infarction and acute myocarditis is promising.

Ischemic heart disease
Differentiation between acute and chronic myocardial infarction has important clinical implications. Late gadolinium enhancement (LGE), which is currently used for the detection of infarcted myocardium, is sensitive to motion-artefacts, and incomplete nulling of the myocardium, and does not differentiate well between acute and chronic myocardial infarction. Early studies using T1 mapping showed that acute and chronic myocardial infarction had different patterns of T1 changes after the administration of gadolinium (43). Besides contrast-enhanced techniques, also native T1 and T2 mapping have shown to be an accurate method for differentiating acute and chronic myocardial infarction via the detection of edema (44, 45). Expansion of current cardiac imaging protocols with T1 and

T2 mapping could thus potentially improve the sensitivity for the detection of myocardial infarction compared to LGE and T2 weighted black blood imaging alone.
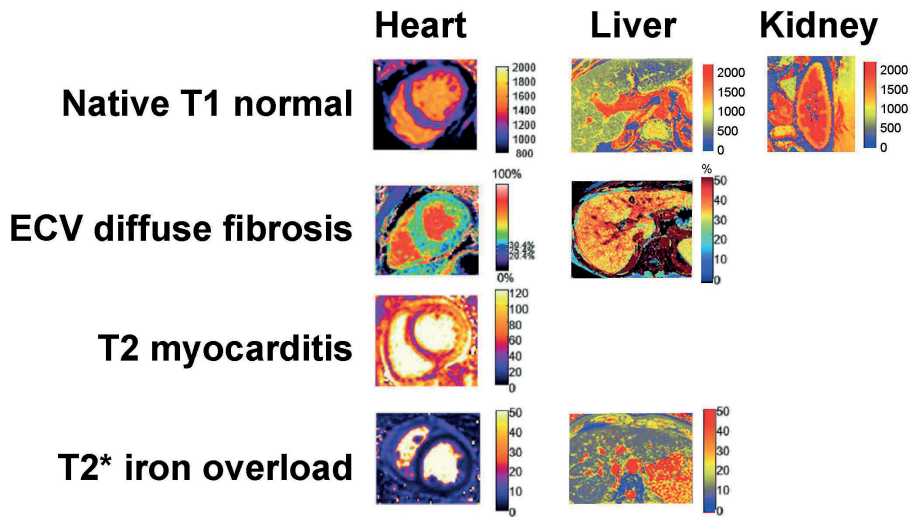
Myocarditis

Acute myocarditis is associated with a high mortality if untreated, however clinical criteria alone are often of limited value for establishing the diagnosis. Both native T1 and T2 mapping have showed to be more sensitive for the detection of acute myocarditis with T2-weighted and LGE MR imaging techniques (46, 47), however native T1 mapping was found to have a superior diagnostic performance compared with T2 mapping (47). Moreover, recent studies have showed that both native T1 mapping and T2 mapping can reliably discriminate between healthy and diseased myocardial tissue (48, 49), and correspond to the clinical disease stage (50). The use of LGE and ECV seems to be beneficial for the detection of more chronic stages of myocarditis (50).

Liver

Estimated annual progression rates of compensated to decompensated liver cirrhosis range between 5 to 11% (51, 52), and prevention of decompensation is the primary treatment goal in compensated cirrhosis (53). However, currently available clinical scoring systems do not accurately identify patients at increased risk of decompensation (54). The observation that the extent of liver enhancement by hepatobiliary specific contrast agents, such as gadobenate dimeglumine and gadoxetate disodium, is liver function dependent has led to multiple studies on contrast-enhanced T1-mapping using these agents. Several of these studies have shown promising results indicating that hepatobiliary contrast enhanced T1-mapping and ECV correlates well with histological measurements of hepatic fibrosis (55), liver function tests (56-60), and Child-Pugh scores (61). Recent studies, however, have indicated that also native hepatic T1 corrected for iron content (cT1) can be used for estimating liver fibrosis (62, 63). cT1 was found to be independently associated with survival in a proof of principle study (64), and was not affected by the degree of adiposity or presence of ascites (62) in contrast to other acoustic-based techniques such as elastography (62). Furthermore, higher liver inflammation and fibrosis scores based on hepatic T1 and T2* values were found to be associated with an increased risk of liver-related adverse outcomes such as encephalopathy, ascites and liver-related death (65).

Already in 2005, it has been described that relaxation rates 1/T2 and 1/T2* could be used as a non-invasive method for the quantification of hepatic iron concentration, as these measures were closely correlated by iron concentration measured via liver biopsy (66). When parametric mapping techniques became available, additional studies histologically validated the ability of T2* mapping for the quantification hepatic iron content (62, 67), and assessed reproducibility (62). A prospective study evaluating the predictive value of T2* on liver-related adverse outcomes found a protective effect with

Figure 7. Typical appearance of T1, T2, T2*, and ECV maps in heart, liver, and kidney of healthy subjects and in patients with myocardial and liver disease. Adapted by permission from BioMed Central under the terms of the Creative Commons License (90), and adapted by permission from BMJ Publishing Group Limited (55).

increasing T2*, which is inversely related to iron load (65). These findings are in line with previous biopsy studies that observed hepatic iron content was predictive of death in alcohol-related liver cirrhosis (68), and more severe fibrosis in non-alcoholic fatty liver disease (69). Non-invasive parametric imaging of the liver could ultimately contribute to personalized medicine based approaches for treatment monitoring, such as evaluating the effects of hepatic iron lowering therapy (**Fig. 6b**) (70) or anti-fibrotic treatment strategies (1). However additional (multicenter) studies are needed in order to determine whether multiparametric MR imaging could indeed contribute to achieving this goal and ultimately replace liver biopsies.

Kidney

On conventional MR imaging of the kidney, anatomical differences between renal cortex and medulla can be clearly differentiated due to the shorter T1 relaxation times of the cortex. Loss of this so-called corticomedullary differentiation occurs in several renal diseases and has been primarily attributed to altered T1 relaxation times in the renal cortex (71). Recent studies suggest that characterization of renal tissue composition via true T1 values without contrast might be useful for differentiating specific renal disease states, such as renal fibrosis imaging. Preclinical studies have shown that T1-mapping could be used for the assessment of acute kidney injury and chronic kidney disease in mice (72-74). Recent clinical studies in renal transplant patients found that renal native T1 values

correlated well with renal fibrosis severity based on histology (75) and with glomerular filtration rate (GFR) after transplantation (76). Good intra- and inter-examination reproducibility has been reported for renal native T1 mapping using the MOLLI 5(3)3 scheme in both healthy human volunteers and diabetic nephropathy patients (77), supporting that native T1 could be used as a reliable and consistent measure of renal tissue composition. However, additional studies are needed to evaluate the reproducibility of renal T1 mapping at different imaging centers with various MRI scanner manufacturers. Since native T1 mapping is at least partially modulated by perfusion (which is also a major determinant of GFR), T1 relaxation times obtained in patients with impaired renal function could theoretically be confounded by lower renal perfusion rather reflecting true fibrosis only. More research is needed to determine to what extent native renal T1 values are affected by impaired perfusion, and whether renal native T1 mapping has added value for clinical decision-making compared to currently available renal function markers and other MR techniques such as diffusion weighted imaging, and blood-oxygen-level dependent imaging. Thus far no studies have evaluated renal extra-cellular (interstitial) volume using native and post-contrast T1-mapping. The administration of contrast in patients with severely impaired renal function is controversial due to the risk of nephrogenic systemic fibrosis (NSF) (78), however new insights suggest that modern macrocyclic GBCAs may not be associated with the development of NSF even when administered to high risk chronic kidney disease patients (79-82). Renal T2 mapping has thus far only been evaluated in mouse models, which showed that renal cortex T2 values increase after kidney transplantation (73) and that renal T2 is highly correlated with the histological cystic index in a polycystic kidney disease model (83). Further research is needed to assess whether T2 mapping could be useful for assessment of edema, or for the prediction of cyst progression in humans.

Technical considerations for clinical implementation

Data acquisition

The decision about the used pulse sequence and parameters starts with the clinical question that needs to be answered, and the disease and organ of interest (**table 2**). Roughly, it can be said that T1 mapping can be used for imaging of fibrosis, steatosis, edema, iron without the need for contrast agents. As native T1 is a measure of both intracellular and extracellular space it is less sensitive to increased extracellular space but more sensitive to other tissue characteristics, such as hemosiderosis, steatosis, and edema. The strength of ECV is; (a) the possibility to differentiate between intracellular versus extra-cellular (interstitial) compartments, and (b) its independence to field strength (84). T2 mapping and T2* mapping are very sensitive for edema and hemosiderosis respectively. Which field strength is optimal for a particular clinical application of T1 and T2(*) mapping is another important question. Most validation studies and references studies for cardiac parametric

imaging have been performed at 1.5T, however most parametric imaging studies of the liver have been performed at 3T. Advantages of higher field strengths are the increased signal to noise ratio, and disadvantages are the larger effects of field inhomogeneities. An overview of the advantages and disadvantages of inversion recovery versus saturation recovery based T1 mapping techniques are presented in **Table 2**.

Table 2. Inversion recovery versus saturation recovery T1-mapping techniques

Technique	Example	Advantages	Disadvantages
Inversion recovery (IR)	MOLLI (1), shMOLLI (2), modified MOLLI	Good precision and reproducibility, few image artefacts	Less absolute accuracy
Saturation recovery (SR)	SASHA (3)	Could potentially provide more accurate T1 measurements, less sensitive to magnetization transfer	More susceptible to noise and artefacts, reproducibility has less extensively been validated
Combined	SAPPHIRE (4)	Shares many of the advantages of IR and SR	Shares the disadvantages of IR

MOLLI, modified look-locker imaging; shMOLLI, shortened MOLLI; SASHA, saturation-recovery single-shot Acquisition; SAPPHIRE, saturation-pulse prepared heart-rate independent inversion-recovery (SAPPHIRE).

Planning

Tissues of interest should be orthogonal to the imaging plane in order to minimize through plane partial volume averaging, which is the two-chamber short axis for the heart, axial for the liver, and axial for the kidney. Furthermore, shimming and center frequency should be adjusted to minimize off resonance, which is especially important at higher field strengths since off-resonance variation may result in regional variations in apparent T1 (85). Adequate breath-holding is needed for correct registration of obtained images, since misregistration can introduce substantial errors in the calculated maps. For cardiac parametric imaging obtained images should be acquired at the same cardiac phase and respiratory position to eliminate tissue motion. Motion-correction could partly overcome the effects of suboptimal breath-holding, and minimize artefacts related to motion and misregistration. The use of fully automated motion correction and co-registration of breath-holds can significantly improve the quality of ECV maps, and increase clinical applicability (86). New developments are the application of 3D imaging and segmentation in order to achieve higher spatial resolution (87), and the use of automated ECV measurement (86) or volumetric ECV measurement for the determination of functional liver-volume (88).

Data analysis and reporting

Clinical imaging units currently provide MR T1 and T2(*) mapping software that can be used for visual evaluation and basic quantification. Post-processing software with dedi-

cated quantification packages are available, which contribute to appropriate scaling of the parametric maps in colour- or grayscale to maximize differentiation between diseased and normal tissues. Regions of interest should be placed with care in order to minimize partial volume effects and should have adequate margins from tissue interfaces, such as the intracardial blood pool, pericardial fat, renal sinus fat and perirenal fat, but also large vascular and biliary structures in the liver. Quantitative error estimates in post-processing software are useful for the assessment of the reliability of measured T1 and T2(*) values. The availability of such quantitative error estimates are an important requirement for the use of quantitative parametric imaging in clinical decision making, since these can help to identify unreliable regions in quantitative imaging and for interpretation and for comparison of imaging protocols (89). The importance of the quality of the pixel-wise T1 and T2(*) maps generated with the chosen pulse sequence, parameters, and field strength cannot be underestimated as for reliable clinical decision making high quality, artefact free pixel-wise maps are crucial (84). The detection of potential artefacts and handling still relies on human expertise, which hampers the easy application of these techniques in clinical practice. The Society for Cardiovascular Magnetic Resonance has recently recommended that local results in healthy volunteers for native T1, and T2 mapping should be primarily used and benchmarked against published reference values (90). For clinical use reference data based on a sufficiently large cohorts reflecting normal variations are needed. Since each T1 and T2(*) mapping technique has specific measurement errors, each technique should in principal be compared with normal reference values that were obtained using the same acquisition method, including same pulse sequence parameters and field strength (84). This requires verification on whether the scanner configurations are identical to the acquisition method used in the reference studies (91). Finally, implementation of T1 and T2(*) mapping results into picture archiving and communication systems could facilitate and enhance the use of parametric imaging data in the clinical work environment.

DISCUSSION

To make the transition from an investigational technique to a reliable clinical modality, T1 and T2(*) mapping studies need to prove that these techniques have the ability to make an early, non-invasive diagnosis or to increase confidence in a suspected diagnosis.

In order for an imaging technique to make a successful transition in clinical setting, the impact of the technique on health care needs to be assessed. Criteria that have been defined to assess the efficacy in diagnostic imaging are; technical feasibility, diagnostic accuracy, diagnostic impact, therapeutic impact, impact on outcome, and societal impact (92). Currently cardiac T1 mapping and hepatic T1 and T2* mapping fulfil the first two cri-

teria, and an increasing amount of studies on cardiac T1 mapping and ECV quantification have demonstrated impact on differential diagnosis, treatment strategies, and clinical outcome. Thus far, only few studies have evaluated societal impact, such as cost-benefit analysis. For multiparametric MR of the liver combined with transient elastography, it has been estimated to yield a cost saving over £500 for every patient needing diagnostic evaluation for non-alcoholic steatohepatitis (93). There is an increasing need for studies evaluating to what extent T1 and T2(*) mapping improve diagnosis and contribute to changes in treatment strategies resulting in improved patient outcomes. In cardiac imaging, T1 values overlap for the majority of cardiac pathologies so its value beyond conventional sequences for diagnostic purposes is remains to be proven. Since hepatic steatosis and siderosis can be easily and accurately quantified by parametric imaging and enable treatment response evaluation, it can expected that T1 and T2* mapping will be increasingly used clinically for liver imaging in the near future. Parametric imaging of the kidney however has just recently entered the research phase. Additional to the above mentioned criteria, more studies are needed to provide good reference data for T1 and T2(*) mapping in order to introduce these techniques into clinical practice.

Ultimately, the intra- and inter-examination reproducibility of measured T1 and T2(*) values determines the clinical utility of pixel-wise T1 and T2(*) mapping for disease assessment. To be of clinical value, assessed experimental and biologic variation in the quantified T1 and T2(*) values should be smaller than the changes caused by disease. In order to assess this, sufficiently large cohorts of subjects are needed to guaranty the robustness of a classifier (e.g. sensitivity and specificity) and ultimately findings should be validated in a multicenter trial. Two large on-going multicenter studies on this topic are currently registered on ClinicalTrials.gov. One will evaluate whether myocardial fibrosis based on LGE and T1 mapping can predict all cause and cardiovascular mortality, with an aimed sample size of 1,500 participants (94). The second study aims investigates whether it is cost-effective to use T1 and T2* imaging of the liver as a standardised diagnostic test for liver disease in 2,000 participants (64). The outcomes of these studies contribute to determining whether parametric imaging will truly find its way into clinical practice, or whether it will remain considered as an 'investigational technique' by medical professionals, and health care institutions.

In conclusion, T1 and T2(*) mapping can be considered promising techniques that can be used in addition to conventional MR imaging for the quantification of pathological changes in tissue composition. Disease entities for which T1 and T2(*) mapping could be used clinically are cardiomyopathies, and ischemic heart disease, and other possible applications are the quantification of liver cirrhosis, hemosiderosis and renal fibrosis. Availability of normative data together with standardization of data acquisition, and analysis is warranted. Multicenter trials with sufficient sample size are needed to establish the impact of T1 and T2(*) mapping on clinical outcome and economic benefit.

REFERENCES

1. Rockey DC, Bell PD, Hill JA. Fibrosis—a common pathway to organ injury and failure. N Engl J Med. 2015;372(12):1138-49.

2. Zeisberg M, Kalluri R. Cellular Mechanisms of Tissue Fibrosis. 1. Common and organ-specific mechanisms associated with tissue fibrosis. Am J Physiol. 2013;304:C216-C25.

3. Scallan J, Huxley V, Korthuis R. Capillary Fluid. Exchange: Regulation, Functions, and Pathology. Integrated Systems Physiology: from Molecule to Function to Disease. San Rafael, CA: Morgan & Claypool Life Sciences; 2010.

4. Abdel-Aty H, Schulz-Menger J. Cardiovascular magnetic resonance T2-weighted imaging of myocardial edema in acute myocardial infarction. Recent Pat Cardiovascular Drug Discov. 2007;2(1):63-8.

5. Pattanayak P, Bleumke DA. Tissue characterization of the myocardium: state of the art characterization by magnetic resonance and computed tomography imaging. Radiol Clin North Am. 2015;53(2):413-23.

6. Spiewak M, Malek LA, Misko J, Chojnowska L, Milosz B, Klopotowski M, et al. Comparison of different quantification methods of late gadolinium enhancement in patients with hypertrophic cardiomyopathy. Eur J Radiol. 2010;74(3):e149-53.

7. Abdel-Aty H, Simonetti O, Friedrich MG. T2-weighted cardiovascular magnetic resonance imaging. J Magn Reson Imaging. 2007;26(3):452-9.

8. Giri S, Chung Y-C, Merchant A, Mihai G, Rajagopalan S, Raman SV, et al. T2 quantification for improved detection of myocardial edema. J Cardiovasc Magn Reson. 2009;11(1):56.

9. Blume U, Lockie T, Stehning C, Sinclair S, Uribe S, Razavi R, et al. Interleaved T1 and T2 relaxation time mapping for cardiac applications. J Magn ResonImaging. 2009;29(2):480-7.

10. Taylor AJ, Salerno M, Dharmakumar R, Jerosch-Herold M. T1 Mapping: Basic Techniques and Clinical Applications. JACC Cardiovasc Imaging. 2016;9(1):67-81.

11. Schelbert EB, Messroghli DR. State of the art: clinical applications of cardiac T1 mapping. Radiology. 2016;278(3):658-76.

12. Messroghli DR, Radjenovic A, Kozerke S, Higgins DM, Sivananthan MU, Ridgway JP. Modified Look-Locker inversion recovery (MOLLI) for high-resolution T1 mapping of the heart. Magn Reson Med. 2004;52(1):141-6.

13. Piechnik SK, Ferreira VM, Dall'Armellina E, Cochlin LE, Greiser A, Neubauer S, et al. Shortened Modified Look-Locker Inversion recovery (ShMOLLI) for clinical myocardial T1-mapping at 1.5 and 3 T within a 9 heartbeat breathhold. J Cardiovasc Magn Reson. 2010;12(1):69.

14. Chow K, Flewitt JA, Green JD, Pagano JJ, Friedrich MG, Thompson RB. Saturation recovery single-shot acquisition (SASHA) for myocardial T1 mapping. Magn Reson Med. 2014;71(6):2082-95.

15. Weingärtner S, Akçakaya M, Basha T, Kissinger KV, Goddu B, Berg S, et al. Combined saturation/inversion recovery sequences for improved evaluation of scar and diffuse fibrosis in patients with arrhythmia or heart rate variability. Magn Reson Med. 2014;71(3):1024-34.

16. Moon JC, Messroghli DR, Kellman P, Piechnik SK, Robson MD, Ugander M, et al. Myocardial T1 mapping and extracellular volume quantification: a Society for Cardiovascular Magnetic Resonance (SCMR) and CMR Working Group of the European Society of Cardiology consensus statement. J Cardiovasc Magn Reson. 2013;15:92.

17. Van Heeswijk RB, Feliciano H, Bongard C, Bonanno G, Coppo S, Lauriers N, et al. Free-breathing 3 T magnetic resonance T 2-mapping of the heart. JACC: Cardiovasc Imaging. 2012;5(12):1231-9.

18. Foltz WD, Al-Kwifi O, Sussman MS, Stainsby JA, Wright GA. Optimized spiral imaging for measurement of myocardial T2 relaxation. Magn Reson Med. 2003;49(6):1089-97.

19. Shah S, Xue H, Greiser A, Weale P, He T, Firmin DN, et al. Inline myocardial t2* mapping with iterative robust fitting. J Cardiovasc Magn Reson. 2011;13(1):P308.

20. Puntmann VO, Peker E, Chandrashekhar Y, Nagel E. T1 Mapping in Characterizing Myocardial Disease: A Comprehensive Review. Circ Res. 2016;119(2):277-99.

21. Jordan JH, Vasu S, Morgan TM, D'Agostino RB, Jr., Melendez GC, Hamilton CA, et al. Anthracycline-Associated T1 Mapping Characteristics Are Elevated Independent of the Presence of Cardiovascular Comorbidities in Cancer Survivors. Circ Cardiovasc Imaging. 2016;9(8).

22. Fontana M, Banypersad SM, Treibel TA, Maestrini V, Sado DM, White SK, et al. Native T1 mapping in transthyretin amyloidosis. JACC Cardiovasc Imaging. 2014;7(2):157-65.

23. Banypersad SM, Fontana M, Maestrini V, Sado DM, Captur G, Petrie A, et al. T1 mapping and survival in systemic light-chain amyloidosis. Eur Heart J. 2014;36(4):244-51.

24. Fontana M, Banypersad SM, Treibel TA, Maestrini V, Sado DM, White SK, et al. Native T1 mapping in transthyretin amyloidosis. JACC Cardiovasc Imaging. 2014;7(2):157-65.

25. Martinez-Naharro A, Kotecha T, Norrington K, Boldrini M, Rezk T, Quarta C, et al. Native T1 and Extracellular Volume in Transthyretin Amyloidosis. JACC Cardiovasc Imaging. 2018 pii: S1936-878X(18)30198-0.

26. Sado DM, White SK, Piechnik SK, Banypersad SM, Treibel T, Captur G, et al. The identification and assessment of Anderson Fabry disease by cardiovascular magnetic resonance non-contrast myocardial T1 mapping. Circ Cardiovasc Imaging. 2013;6(3):392-8.

27. Sado DM, Maestrini V, Piechnik SK, Banypersad SM, White SK, Flett AS, et al. Noncontrast myocardial T1 mapping using cardiovascular magnetic resonance for iron overload. J Magn Reson Imaging. 2015;41(6):1505-11.

28. Kuruvilla S, Janardhanan R, Antkowiak P, Keeley EC, Adenaw N, Brooks J, et al. Increased extracellular volume and altered mechanics are associated with LVH in hypertensive heart disease, not hypertension alone. JACC Cardiovasc Imaging. 2015;8(2):172-80.

29. Nakamori S, Dohi K, Ishida M, Goto Y, Imanaka-Yoshida K, Omori T, et al. Native T1 Mapping and Extracellular Volume Mapping for the Assessment of Diffuse Myocardial Fibrosis in Dilated Cardiomyopathy. JACC Cardiovasc Imaging. 2018;11(1):48-59.

30. Carpenter J-P, He T, Kirk P, Roughton M, Anderson LJ, de Noronha SV, et al. On T2* Magnetic Resonance and Cardiac Iron. Circulation. 2011;123(14):1519-28.

31. Hur DJ, Dicks DL, Huber S, Mojibian HR, Meadows JL, Seropian SE, et al. Serial Native T1 Mapping to Monitor Cardiac Response to Treatment in Light-Chain Amyloidosis. Circ Cardiovasc Imaging. 2016;9(10).

32. Messalli G, Imbriaco M, Avitabile G, Russo R, Iodice D, Spinelli L, et al. Role of cardiac MRI in evaluating patients with Anderson-Fabry disease: assessing cardiac effects of long-term enzyme replacement therapy. Radiol Med. 2012;117(1):19-28.

33. Modell B, Khan M, Darlison M, Westwood MA, Ingram D, Pennell DJ. Improved survival of thalassaemia major in the UK and relation to T2* cardiovascular magnetic resonance. J Cardiovasc Magn Reson. 2008;10:42.

34. Stuckey DJ, McSweeney SJ, Thin MZ, Habib J, Price AN, Fiedler LR, et al. T(1) mapping detects pharmacological retardation of diffuse cardiac fibrosis in mouse pressure-overload hypertrophy. Circ Cardiovasc Imaging. 2014;7(2):240-9.

35. Jerosch-Herold M, Sheridan DC, Kushner JD, Nauman D, Burgess D, Dutton D, et al. Cardiac magnetic resonance imaging of myocardial contrast uptake and blood flow in patients affected with idiopathic or familial dilated cardiomyopathy. Am J Physiol Heart Circ Physiol. 2008;295(3):H1234-H42.

36. Su M-YM, Lin L-Y, Tseng Y-HE, Chang C-C, Wu C-K, Lin J-L, et al. CMR-verified diffuse myocardial fibrosis is associated with diastolic dysfunction in HFpEF. JACC Cardiovasc Imaging. 2014;7(10):991-7.

37. Adam RD, Shambrook J, Flett AS. The Prognostic Role of Tissue Characterisation using Cardiovascular Magnetic Resonance in Heart Failure. Cardiac Fail Rev. 2017;3(2):86-96.

38. Mascherbauer J, Marzluf BA, Tufaro C, Pfaffenberger S, Graf A, Wexberg P, et al. Cardiac magnetic resonance postcontrast T1 time is associated with outcome in patients with heart failure and preserved ejection fraction. Circ Cardiovasc Imaging. 2013;6(6):1056-65.

39. Puntmann VO, Carr-White G, Jabbour A, Yu CY, Gebker R, Kelle S, et al. T1-Mapping and Outcome in Nonischemic Cardiomyopathy: All-Cause Mortality and Heart Failure. JACC Cardiovasc imaging. 2016;9(1):40-50.

40. Youn JC, Hong YJ, Lee HJ, Han K, Shim CY, Hong GR, et al. Contrast-enhanced T1 mapping-based extracellular volume fraction independently predicts clinical outcome in patients with non-ischemic dilated cardiomyopathy: a prospective cohort study. Eur Radiol. 2017;27(9):3924-33.

41. Duca F, Kammerlander AA, Zotter-Tufaro C, Aschauer S, Schwaiger ML, Marzluf BA, et al. Interstitial Fibrosis, Functional Status, and Outcomes in Heart Failure With Preserved Ejection Fraction: Insights From a Prospective Cardiac Magnetic Resonance Imaging Study. Circ Cardiovasc Imaging. 2016;9(12).

42. Barison A, Del Torto A, Chiappino S, Aquaro GD, Todiere G, Vergaro G, et al. Prognostic significance of myocardial extracellular volume fraction in nonischaemic dilated cardiomyopathy. J Cardiovasc Med. 2015;16(10):681-7.

43. Messroghli DR, Walters K, Plein S, Sparrow P, Friedrich MG, Ridgway JP, et al. Myocardial T1 mapping: application to patients with acute and chronic myocardial infarction. Magn Reson Med. 2007;58(1):34-40.

44. Ugander M, Bagi PS, Oki AJ, Chen B, Hsu L-Y, Aletras AH, et al. Myocardial edema as detected by pre-contrast T1 and T2 CMR delineates area at risk associated with acute myocardial infarction. JACC: Cardiovasc Imaging. 2012;5(6):596-603.

45. Tahir E, Sinn M, Bohnen S, Avanesov M, Säring D, Stehning C, et al. Acute versus Chronic Myocardial Infarction: Diagnostic Accuracy of Quantitative Native T1 and T2 Mapping versus Assessment of Edema on Standard T2-weighted Cardiovascular MR Images for Differentiation. Radiology. 2017:162338.

46. Thavendiranathan P, Walls M, Giri S, Verhaert D, Rajagopalan S, Moore S, et al. Improved detection of myocardial involvement in acute inflammatory cardiomyopathies using T2 mapping. Circ Cardiovasc Imaging. 2012;5(1):102-10.

47. Ferreira VM, Piechnik SK, Dall'Armellina E, Karamitsos TD, Francis JM, Ntusi N, et al. T 1 Mapping for the Diagnosis of Acute Myocarditis Using CMR. JACC Cardiovasc Imaging. 2013;6(10):1048-58.

48. Hinojar R, Foote L, Ucar EA, Jackson T, Jabbour A, Yu C-Y, et al. Native T1 in discrimination of acute and convalescent stages in patients with clinical diagnosis of myocarditis: a proposed diagnostic algorithm using CMR. JACC Cardiovasc Imaging. 2015;8(1):37-46.

49. von Knobelsdorff-Brenkenhoff F, Schüler J, Dogangüzel S, Dieringer MA, Rudolph A, Greiser A, et al. Detection and Monitoring of Acute Myocarditis Applying Quantitative Cardiovascular Magnetic Resonance. Circ Cardiovasc Imaging. 2017;10(2).

50. Bohnen S, Radunski U, Lund G, Ojeda F, Looft Y, Senel M, et al. Tissue characterization by T1 and T2 mapping cardiovascular magnetic resonance imaging to monitor myocardial inflammation in healing myocarditis. Eur Heart J Cardiovasc Imaging. 2017;18(7):744-751.

51. D'Amico G, Garcia-Tsao G, Pagliaro L. Natural history and prognostic indicators of survival in cirrhosis: a systematic review of 118 studies. J Hepatol. 2006;44(1):217-31.

52. Fleming KM, Aithal G, Card T, West J. The rate of decompensation and clinical progression of disease in people with cirrhosis: a cohort study. Alimen Pharmacol Ther. 2010;32(11-12):1343-50.

53. Garcia-Tsao G, Lim J. Management and treatment of patients with cirrhosis and portal hypertension: recommendations from the Department of Veterans Affairs Hepatitis C Resource Center Program and the National Hepatitis C Program. Am J Gastroenterol. 2009;104(7):1802.

54. Garcia-Tsao G, Friedman S, Iredale J, Pinzani M. Now there are many (stages) where before there was one: In search of a pathophysiological classification of cirrhosis. Hepatology. 2010;51(4):1445-9.

55. Luetkens JA, Klein S, Traeber F, Schmeel FC, Sprinkart AM, Kuetting DLR, et al. Quantitative liver MRI including extracellular volume fraction for non-invasive quantification of liver fibrosis: a prospective proof-of-concept study. Gut. 2018;67(3):593-4.

56. Katsube T, Okada M, Kumano S, Hori M, Imaoka I, Ishii K, et al. Estimation of liver function using T1 mapping on Gd-EOB-DTPA-enhanced magnetic resonance imaging. Invest Radiol. 2011;46(4):277-83.

57. Haimerl M, Verloh N, Zeman F, Fellner C, Müller-Wille R, Schreyer AG, et al. Assessment of clinical signs of liver cirrhosis using T1 mapping on Gd-EOB-DTPA-enhanced 3T MRI. PloS One. 2013;8(12):e85658.

58. Ding Y, Rao S-X, Chen C, Li R, Zeng M-S. Assessing liver function in patients with HBV-related HCC: a comparison of T1 mapping on Gd-EOB-DTPA-enhanced MR imaging with DWI. Eur Radiol. 2015;25(5):1392-8.

59. Ding Y, Rao S-X, Zhu T, Chen C-Z, Li R-C, Zeng M-S. Liver fibrosis staging using T1 mapping on gadoxetic acid-enhanced MRI compared with DW imaging. Clin Radiol. 2015;70(10):1096-103.

60. Besa C, Bane O, Jajamovich G, Marchione J, Taouli B. 3D T1 relaxometry pre and post gadoxetic acid injection for the assessment of liver cirrhosis and liver function. Magn Reson Imaging. 2015;33(9):1075-82.

61. Yoon JH, Lee JM, Paek M, Han JK, Choi BI. Quantitative assessment of hepatic function: modified look-locker inversion recovery (MOLLI) sequence for T1 mapping on Gd-EOB-DTPA-enhanced liver MR imaging. Eur Radiol. 2016;26(6):1775-82.

62. Banerjee R, Pavlides M, Tunnicliffe EM, Piechnik SK, Sarania N, Philips R, et al. Multiparametric magnetic resonance for the non-invasive diagnosis of liver disease. J Hepatol. 2014;60(1):69-77.

63. Cassinotto C, Feldis M, Vergniol J, Mouries A, Cochet H, Lapuyade B, et al. MR relaxometry in chronic liver diseases: Comparison of T1 mapping, T2 mapping, and diffusion-weighted imaging for assessing cirrhosis diagnosis and severity. Eur J Radiol. 2015;84(8):1459-65.

64. Clinicaltrials.gov [homepage on the internet] Non-Invasive Rapid Assessment of Patients With Liver Transplants Using Magnetic Resonance Imaging With LiverMultiScan (RADIcAL2) [updated 2017 September 19; cited 2018 April 28]. Available from: https://clinicaltrials.gov/ct2/show/NCT03165201?term=LiverMultiScan&rank=1: ClinicalTrials.gov.

65. Pavlides M, Banerjee R, Sellwood J, Kelly CJ, Robson MD, Booth JC, et al. Multiparametric magnetic resonance imaging predicts clinical outcomes in patients with chronic liver disease. J Hepatol. 2016;64(2):308-15.

66. Wood JC, Enriquez C, Ghugre N, Tyzka JM, Carson S, Nelson MD, et al. MRI R2 and R2* mapping accurately estimates hepatic iron concentration in transfusion-dependent thalassemia and sickle cell disease patients. Blood. 2005;106(4):1460-5.

67. Henninger B, Kremser C, Rauch S, Eder R, Zoller H, Finkenstedt A, et al. Evaluation of MR imaging with T1 and T2* mapping for the determination of hepatic iron overload. Eur Radiol. 2012;22(11):2478-86.

68. Ganne-Carrié N, Christidis C, Chastang C, Ziol M, Chapel F, Imbert-Bismut F, et al. Liver iron is predictive of death in alcoholic cirrhosis: a multivariate study of 229 consecutive patients with alcoholic and/or hepatitis C virus cirrhosis: a prospective follow up study. Gut. 2000;46(2):277-82.

69. Valenti L, Fracanzani AL, Bugianesi E, Dongiovanni P, Galmozzi E, Vanni E, et al. HFE Genotype, Parenchymal Iron Accumulation, and Liver Fibrosis in Patients With Nonalcoholic Fatty Liver Disease. Gastroenterology. 2010;138(3):905-12.

70. Fischer R, Piga A, Harmatz P, Nielsen P. Monitoring long-term efficacy of iron chelation treatment with biomagnetic liver susceptometry. Ann N Y Acad Sci. 2005;1054:350-7.

71. Lee VS, Kaur M, Bokacheva L, Chen Q, Rusinek H, Thakur R, et al. What causes diminished corticomedullary differentiation in renal insufficiency? J Magn Reson Imaging. 2007;25(4):790-5.

72. Hueper K, Peperhove M, Rong S, Gerstenberg J, Mengel M, Meier M, et al. T1-mapping for assessment of ischemia-induced acute kidney injury and prediction of chronic kidney disease in mice. Eur Radiol. 2014;24(9):2252-60.

73. Hueper K, Hensen B, Gutberlet M, Chen R, Hartung D, Barrmeyer A, et al. Kidney Transplantation: Multiparametric Functional Magnetic Resonance Imaging for Assessment of Renal Allograft Pathophysiology in Mice. Invest Radiol. 2016;51(1):58-65.

74. Tewes S, Gueler F, Chen R, Gutberlet M, Jang M-S, Meier M, et al. Functional MRI for characterization of renal perfusion impairment and edema formation due to acute kidney injury in different mouse strains. PLOS One. 2017;12(3):e0173248.

75. Friedli I, Crowe LA, Berchtold L, Moll S, Hadaya K, de Perrot T, et al. New Magnetic Resonance Imaging Index for Renal Fibrosis Assessment: A Comparison between Diffusion-Weighted Imaging and T1 Mapping with Histological Validation. Sci Rep. 2016;6:30088.

76. Peperhove M, Vo Chieu VD, Jang MS, Gutberlet M, Hartung D, Tewes S, et al. Assessment of acute kidney injury with T1 mapping MRI following solid organ transplantation. Eur Radiol. 2017.

77. Reproducibility of Native T1 Mapping for Renal Tissue Characterization at 3T. Dekkers IA, Paiman EHM, de Vries APJ, Lamb HJ. J Magn Reson Imaging. 2019 Feb;49(2):588-96.78.   Perazella   MA. Gadolinium-contrast toxicity in patients with kidney disease: nephrotoxicity and nephrogenic systemic fibrosis. Curr Drug Saf. 2008;3(1):67-75.

79. Martin DR, Kalb B, Mittal A, Salman K, Vedantham S, Mittal PK. No Incidence of Nephrogenic Systemic Fibrosis after Gadobenate Dimeglumine Administration in Patients Undergoing Dialysis or Those with Severe Chronic Kidney Disease. Radiology. 2017;0(0):170102.

80. Soulez G, Bloomgarden DC, Rofsky NM, Smith MP, Abujudeh HH, Morgan DE, et al. Prospective cohort study of nephrogenic systemic fibrosis in patients with stage 3–5 chronic kidney disease undergoing MRI with injected gadobenate dimeglumine or gadoteridol. AJR Am J Roentgenol. 2015;205(3):469-78.

81. Bruce R, Wentland AL, Haemel AK, Garrett RW, Sadowski DR, Djamali A, et al. Incidence of nephrogenic systemic fibrosis using gadobenate dimeglumine in 1423 patients with renal insufficiency compared with gadodiamide. Invest Radiol. 2016;51(11):701-5.

82. Michaely HJ, Aschauer M, Deutschmann H, Bongartz G, Gutberlet M, Woitek R, et al. Gadobutrol in renally impaired patients: results of the GRIP Study. Invest Radiol. 2017;52(1):55.

83. Franke M, Baessler B, Vechtel J, Dafinger C, Hohne M, Borgal L, et al. Magnetic resonance T2 mapping and diffusion-weighted imaging for early detection of cystogenesis and response to therapy in a mouse model of polycystic kidney disease. Kidney Int. 2017.

84. Kellman P, Hansen MS. T1-mapping in the heart: accuracy and precision. J Cardiovasc Magn Reson. 2014;16:2.

85. Kellman P, Herzka DA, Arai AE, Hansen MS. Influence of Off-resonance in myocardial T1-mapping using SSFP based MOLLI method. J Cardiovasc Magn Reson. 2013;15(1):63.

86. Kellman P, Wilson JR, Xue H, Ugander M, Arai AE. Extracellular volume fraction mapping in the myocardium, part 1: evaluation of an automated method. J Cardiovasc Magn Reson. 2012;14(1):63.

87. Kvernby S, Warntjes MJB, Haraldsson H, Carlhäll C-J, Engvall J, Ebbers T. Simultaneous three-dimensional myocardial T1 and T2 mapping in one breath hold with 3D-QALAS. J Cardiovasc Magn Reson. 2014;16(1):102.

88. Yoon JH, Lee JM, Kim E, Okuaki T, Han JK. Quantitative Liver Function Analysis: Volumetric T1 Mapping with Fast Multisection B1 Inhomogeneity Correction in Hepatocyte-specific Contrast-enhanced Liver MR Imaging. Radiology. 2016;282(2):408-17.

89. Sandino CM, Kellman P, Arai AE, Hansen MS, Xue H. Myocardial T2* mapping: influence of noise on accuracy and precision. J Cardiovasc Magn Reson. 2015;17(1):7.

90. Messroghli DR, Moon JC, Ferreira VM, Grosse-Wortmann L, He T, Kellman P, et al. Clinical recommendations for cardiovascular magnetic resonance mapping of T1, T2, T2* and extracellular volume: A consensus statement by the Society for Cardiovascular Magnetic Resonance (SCMR) endorsed by the European Association for Cardiovascular Imaging (EACVI). J Cardiovasc Magn Reson. 2017;19(1):75.

91. Moon JC, Messroghli DR, Kellman P, Piechnik SK, Robson MD, Ugander M, et al. Myocardial T1 mapping and extracellular volume quantification: a Society for Cardiovascular Magnetic Resonance (SCMR) and CMR Working Group of the European Society of Cardiology consensus statement. J Cardiovasc Magn Reson. 2013;15(1):92.

92. Fryback DG, Thornbury JR. The efficacy of diagnostic imaging. Med Decis Making. 1991;11(2):88-94.

93. Blake L, Duarte RV, Cummins C. Decision analytic model of the diagnostic pathways for patients with suspected non-alcoholic fatty liver disease using non-invasive transient elastography and multiparametric magnetic resonance imaging. BMJ open. 2016;6(9):e010507.

94. Clinicaltrials.gov [homepage on the internet] International T1 Multicenter CMR Outcome Study in Patients With Nonischaemic Cardiomyopathies (T1-CMR). [updated 2015 April 2; cited 2018 April 28]. Available from: https://clinicaltrials.gov/ct2/show/NCT02407197

95. Haaf P, Garg P, Messroghli DR, Broadbent DA, Greenwood JP, Plein S. Cardiac T1 Mapping and Extracellular Volume (ECV) in clinical practice: a comprehensive review. J Cardiovasc Magn Reson. 2016;18(1):89.